


## RESEARCH ARTICLE

# Estimation of abnormal wave propagation by a novel duct map based on the average normalized path loss

Sungsik Wang<sup>1</sup> | Tae H. Lim<sup>1</sup> |  
Young J. Chong<sup>2</sup> | Jinwon Ko<sup>3</sup> |  
Yong B. Park<sup>4</sup> | Hosung Choo<sup>1</sup> 

<sup>1</sup>School of Electronic and Electrical Engineering, Hongik University, Seoul, South Korea

<sup>2</sup>Telecommunications & Media Research Laboratory, Electronics and Telecommunications Research Institute, Daejeon, South Korea

<sup>3</sup>AESA Radar R&D Center, Hanwha Systems, Yongin, Gyeonggi, South Korea

<sup>4</sup>Department of Electrical and Computer Engineering, Ajou University, Suwon, South Korea

## Correspondence

Hosung Choo, School of Electronic and Electrical Engineering, Hongik University, 94, Wausan-ro, Mapo-gu, Seoul, 04066, South Korea.  
Email: hschoo@hongik.ac.kr

## Funding information

HANWHA SYSTEMS; Ministry of Science, ICT and Future Planning, Grant/Award Number: 2017-0-00066

## Abstract

In this paper, the path losses between the Jeungdo and Heuksando transceivers located in the coastal areas of Korea are studied using the Advanced Refractive Prediction System simulation software based on the actual coastal weather database. Based on the simulated data, we propose a novel duct map that can effectively estimate the abnormal wave propagation characteristics by using the atmospheric refractive index dependent on altitude as well as the location parameters of Rx and Tx. To verify the proposed duct map, two representative atmospheric index samples are obtained from the 2017 weather database of the Heuksando weather forecast station, causing the abnormal path loss characteristics. The simulated path losses for abnormal conditions at the Rx point are 132.3 and 140.1 dB, respectively, and these results demonstrate that the abnormal radio wave propagation can effectively be predicted through the proposed duct map.

## KEYWORDS

duct, propagation interference, refractive index, trilinear modeling

## 1 | INTRODUCTION

With the dramatic improvement of wireless communication technologies, the use of radio frequency in a limited frequency bandwidth has been growing explosively.<sup>1,2</sup> Even though a variety of techniques, such as cell-to-cell distance adjustment and cell-to-cell frequency redistribution, are employed for this purpose, such dense frequency usage in a limited bandwidth increases the unintentional radio interference between the local base stations, transceivers located at long distances, and even broadcasts in some countries.<sup>3</sup> Generally, abnormal radio interference is often caused by various wave propagation characteristics, such as external noise, clutter, atmospheric gas, vapor, multi-path polarization, scattering, and changes in the atmosphere refractive index.<sup>4-6</sup> Among these various phenomena that result in radio interferences, the abnormal refractive index from the atmospheric conditions can, in particular, have an unintended interference effect on long-distance communications.<sup>5,6</sup> The index of refraction in the atmosphere represents the degree of directional bending during wave propagation in the medium, which is determined by the atmospheric gas pressure, relative humidity, and temperature, varying according to the location and height in the troposphere.<sup>6-8</sup> The vertical variation of the refractivity is a predominant factor affecting the wave propagation characteristics, and four types of refractive conditions, such as sub, super, normal, and duct, are determined depending on the gradient value of the refractivity index.<sup>9-15</sup>

Among these, the duct is the most significant influencing factor for long-range radio interference.<sup>11</sup> Ducting acts as a waveguide for the electromagnetic (EM) waves due to its negative gradient refractivity index with respect to altitude.<sup>6</sup> Although the ducts in general have a significant impact on the radar and communication systems operating in the microwave range, if the antennas are not in specific positions in the duct, then it would not be a major radio interference factor. For example, it has been reported that the path loss is about 20-30 dB lower when the receiving antenna is located inside the duct in comparison to when it is located just outside of it.<sup>12</sup> This implies that the relative positions of the

transmitting antenna (Tx) and receiving antenna (Rx) with respect to the height and thickness of the duct have a significant influence on the radio interference.<sup>16</sup> Thus, in order to predict the abnormal variation of the path loss or the propagation factor due to the ducting, the atmospheric refraction index, as well as the location parameters of the Tx and Rx, should be carefully considered.

An atmospheric refractive index that is similar to that found in normal conditions is typically modeled as an exponential function of height,<sup>14</sup> but it is not suitable for duct modeling due to an abnormal atmospheric phenomenon that occurs only for a short time, unlike a standard one. Therefore, trilinear modeling has been proposed and widely used for duct modeling.<sup>10</sup> Recently, Karimian et al used trilinear modeling to estimate the low-altitude atmospheric refractivity index from a given wave propagation loss measurement,<sup>5</sup> and the refractivity index was modeled from the actual local measurement meteorological data.<sup>17</sup> Some studies in the UAE used the local radiosonde data for 17 years to obtain a vertical refractivity index profile for three critical atmospheric layers.<sup>9</sup> For coastal areas in UAE,<sup>9</sup> North America,<sup>16</sup> China,<sup>12</sup> and Australia,<sup>18</sup> there have been several studies of ducts that use the atmospheric refractive index from the weather forecast database and measurements for their path loss analysis. Statistical analysis was also introduced for the interpretation of the measured data.<sup>5</sup> However, most previous research focused only on the effect of the duct refractive index on wave propagation, while the relationship between the position parameters (the heights of the Rx and Tx) and the abnormal wave propagation in ducting atmospheric conditions has not been fully studied yet.

In this paper, the propagation path losses between the Jeungdo and Heuksando transceivers located in the coastal areas of Korea are investigated using the Advanced Refractive Prediction System (AREPS) simulation software<sup>20</sup> based on the actual coastal weather database. Then, a novel duct map is proposed here to effectively estimate the abnormal wave propagation characteristics according to the

altitude refractive index, as well as to the location parameters of the Tx and Rx. The atmospheric refractive index dependent on altitude is achieved using the database of the Heuksando weather forecast station, and the digital terrain elevation data (DTED) was used for the AREPS simulation condition.

Subsequently, simple trilinear modeling is employed to model the modified refractive indices for various ducts, and this model can be categorized according to the characteristics of the ducting conditions, such as its occurring height and thickness. In our duct map, trilinear modeling for duct conditions can be divided into several different situations according to the height parameters of the Rx and Tx. In particular, the proposed duct map employs an average normalized path loss in order to examine the influence of the duct on wave propagation more clearly. Through the developed duct map, the duct types that cause the most abnormal wave propagation in given Tx and Rx conditions are determined. In order to validate the proposed duct map, two different refractive indices are obtained from the 2017 weather database, which are causing the abnormal path loss characteristics. With these real atmospheric conditions and the DTED between the Jeungdo and Heuksando, the path loss simulations are conducted using the AREPS simulation software. The results confirm that abnormal radio wave propagation can be predicted through the observation of the proposed duct map and that significantly different path loss characteristics are achieved depending on the height parameters of Tx and Rx in comparison to the altitude of the duct.

## 2 | WAVE PROPAGATION IN MEASUREMENT

Figure 1 shows wave propagations with the sub, normal, and super refraction, as well as the trap, according to the gradient of modified refractive index  $M$  in terms of heights. The

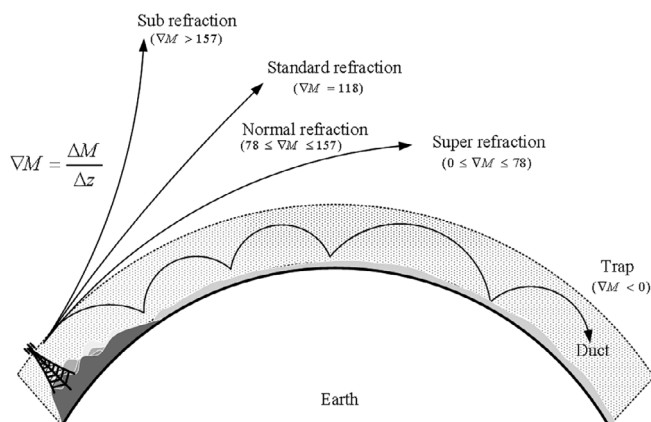


**FIGURE 1** Wave propagations according to the gradient of modified refractive index  $M$  in terms of heights

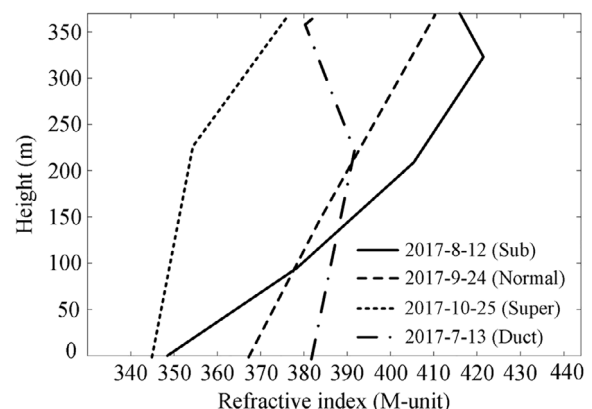


**FIGURE 2** Modified atmospheric refractivity according to altitude at the Heuksando meteorological observatory

modified refractive index  $M$  is defined by adding the ratio of the height  $h$  (m) to the earth's curvature as follows<sup>12</sup>:

$$M = (n-1) \times 10^6 + 0.157h, \quad (1)$$

The sub refraction ( $\nabla M \geq 157$ ) indicates that the wave becomes extremely bent in the direction opposite to the earth's surface, in which the gradient of  $M$  is larger than that of the normal refraction ( $78 \leq \nabla M \leq 157$ ). On the other hand, when the gradient of  $M$  turns into a smaller than normal refraction, the wave bend toward the earth's surface, which is called the super refraction ( $0 \leq \nabla M \leq 78$ ). Moreover, when the gradient of  $M$  becomes negative, a duct or trap phenomenon occurs as if wave propagation is trapped in a waveguide.<sup>10</sup>

Figure 2 shows the modified refractive index data of the sub, normal, super, and duct refraction along with the altitude extracted from the 2017 weather database of the Heuksando meteorological station. The solid line indicates the sub refractive index ( $141 \leq \nabla M \leq 315$ ) up to a height of 323 m on August 12, and the normal refractive index ( $110 \leq \nabla M \leq 125$ ) was found on September 24, shown as a dashed line. The super refractive index ( $\nabla M \leq 42$ ) up to a height of 230 m was observed on October 25, specified by a dashed line. The elevated duct environment was monitored above the altitude of 225 m on July 13th, as indicated with a dash-dot line. The duct atmospheric data is essential for examining an abnormal propagation phenomenon where the path loss suddenly decreases or increases at the Rx in comparison to the normal atmospheric condition. The detailed values for the modified refractive index of the simulation are listed in Table 1, where  $h$  is the height. Figure 3A illustrates the wave propagation model to be analyzed including atmospheric conditions, antenna patterns, frequency, and the terrain elevation information of the Jeungdo-Heuksando area in Korea. The Tx is located at the height of  $h_{Tx}$  with an omni-

**TABLE 1** Modified refractive index under 400 m

Date	Atmospheric condition	Refractive index gradient
July 13, 2017	Elevated duct	$\nabla M = 46$ ( $0 \leq h \leq 225$ m) $\nabla M = -86$ ( $225 \text{ m} \leq h \leq 361$ m) $\nabla M = 265$ ( $362 \leq h$ )
August 12, 2017	Sub	$\nabla M = 315$ ( $0 \leq h \leq 95$ m) $\nabla M = 236$ ( $96 \text{ m} \leq h \leq 209$ m) $\nabla M = 141$ ( $210 \text{ m} \leq h$ )
September 24, 2017	Normal	$\nabla M = 110$ ( $0 \leq h \leq 148$ m) $\nabla M = 120$ ( $149 \text{ m} \leq h \leq 372$ m) $\nabla M = 125$ ( $373 \text{ m} \leq h$ )
October 25, 2017	Super	$\nabla M = 42$ ( $0 \leq h \leq 228$ m) $\nabla M = 155$ ( $229 \text{ m} \leq h$ )

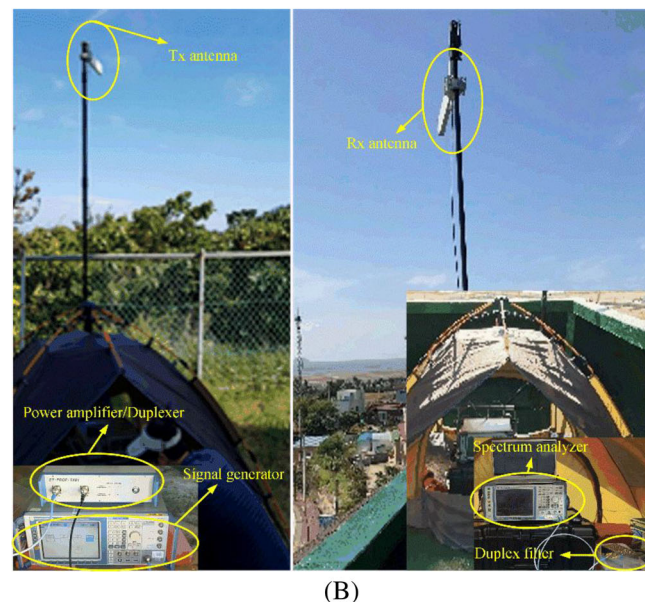
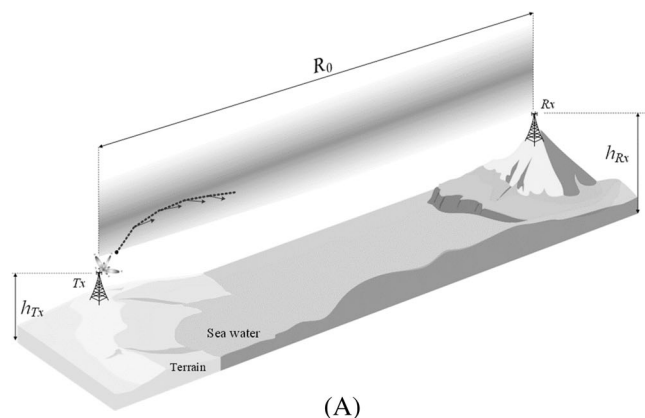


**FIGURE 3** Wave propagation model of the Jeungdo-Heuksando area in Korea. A, Wave propagation model. B, Measurement setup [Color figure can be viewed at [wileyonlinelibrary.com](http://wileyonlinelibrary.com)]

directional antenna, and the path loss is observed from the Rx at the altitude of  $h_{Rx}$ , where the distance between the Tx and Rx is  $R_0$ . If antennas with more directivity are used, we could have the higher received power (increased by Rx and Tx antenna gains) and lower fluctuating path loss amplitude due to the lower ground reflections. To simulate for actual atmospheric conditions, the refractive index was extracted from the 2017 weather database of the Heuksando meteorological station using information of atmospheric pressure, temperature, and relative humidity according to height, and the detailed parameters for these conditions are listed in Table 2. The AREPS commercial EM software,<sup>20</sup> a well-known simulation software, is used for EM numerical simulations to calculate the path loss considering these conditions, and the accuracy of the software has been proven by several previous studies.<sup>22</sup> There are more tools that allow similar numerical simulation results, such as Integrated Refraction Effects Prediction System (IREPS), Engineer's Refractive Effects Prediction System (EREPS), Tactical Electronic Support System (TESS), Advanced Refractive Effects Prediction System (AREPS), Tropospheric



**TABLE 2** Modeling parameters

Parameter	$h_{Rx}$	$h_{Tx}$	$R_0$	Antenna pattern	Frequency	Tool
Value	249 m (Heuksando)	100 m (Jeungdo)	78 km	Omni-directional Vertical polarization	2.85 GHz	AREPS

Abbreviation: Advanced Refractive Prediction System.

**TABLE 3** System parameters for the experimental measurement

System parameter	Rx antenna gain	Tx antenna gain	Total Tx power	Antenna bandwidth
Value	10 dBi at 2.85 GHz	10 dBi at 2.85 GHz	53.56 dBm	980 MHz (1710–2690 MHz)

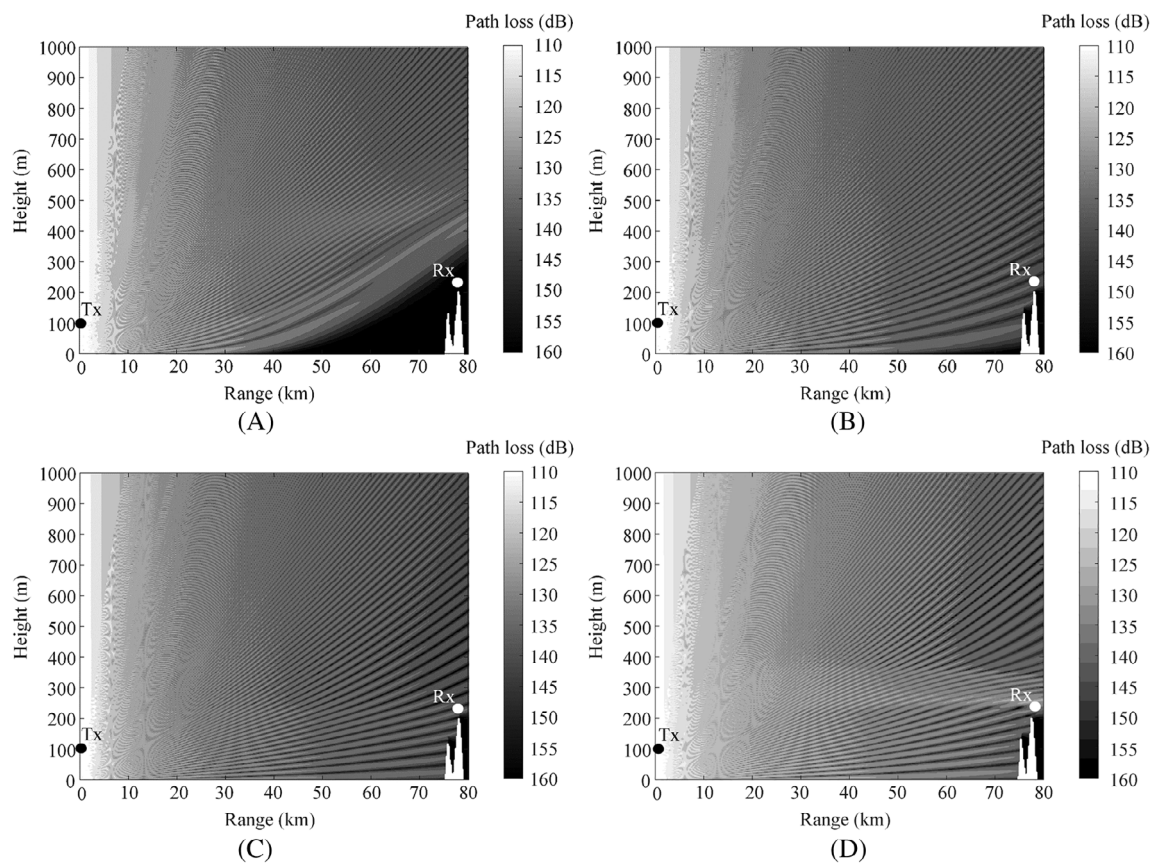


**FIGURE 4** Simulation path losses resulting from the four measured atmospheric data. A, 2017-8-12-00 (sub type). B, 2017-9-24-00 (normal type). C, 2017-10-25-00 (super type). D, 2017-7-13-00 (duct type)

Electromagnetic Parabolic Equation Routine (TEMPER), Terrain Parabolic Equation Model (TPEM), and Parabolic Equation Toolbox for matlab (PETOOL).<sup>21,22</sup> Figure 3B illustrates the measurement setup. The Tx system consists of a signal generator (ROHDE&SCHWARZ R&S SMW200A, 0 dBm), a power amplifier (45 dB) with a duplexer, Tx-cables (−1.44 dB), and an antenna (10 dBi) having 980 a bandwidth of 980 MHz at 2.85 GHz. The Rx system consists of a spectrum analyzer (ROHDE&SCHWARZ R&S FSVR), a duplexer filter (−0.8 dB), Rx-cables (−1.44 dB), and the same antenna with Tx. The detailed parameters are listed in Table 3. To compensate for the simulation condition, the total antenna gain of 20 dB is subtracted from the measured Tx to Rx results.

Figure 4 demonstrates the simulation path losses applying the four measured atmospheric data (sub, normal, super, and duct) to the above conditions. Since the wave propagation is bent upward in the vicinity of the Rx point, as shown in Figure 4A, the path loss of 162.8 dB is obtained with the sub atmospheric condition on August 12. Figure 4B, C present the path losses for the normal and super wave propagations using the atmospheric data of September 24 and October 25, respectively. The super refraction causes the wave propagation to bend toward the ground, resulting in a path loss of 139.2 dB at the Rx point, which is 4.9 dB lower than the normal atmosphere. The elevated duct is a special case of wave propagation by the negative  $\nabla M$  in which the strong energy is confined in

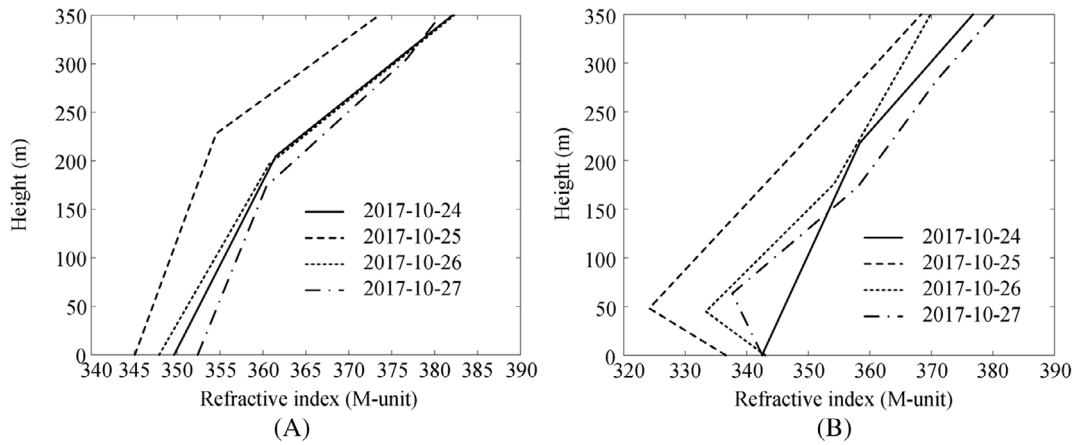


**FIGURE 5** Modified atmospheric refractivity of the Heuksando Rx station. A, Modified atmospheric refractivity according to altitude at the Heuksando meteorological observatory at 0:00 AM in October 2017. B, Modified atmospheric refractivity according to altitude at the Heuksando meteorological observatory at 12:00 PM in October 2017

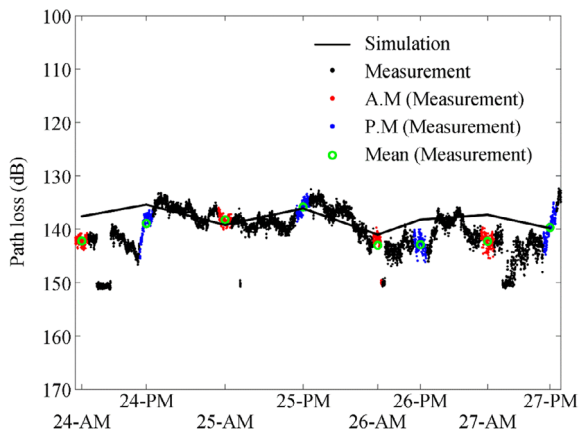


**FIGURE 6** Measured and simulated results of the path loss at the Heuksando Rx station in October 2017 [Color figure can be viewed at wileyonlinelibrary.com]

the duct causing a lowest path loss of 133.6 dB at the Rx point, as represented in Figure 4D.

Figure 5A presents the modified refractive indices at 0:00 AM gathered from the weather database at the Heuksando meteorological observatory in the dates from October 24 to 27, 2017, and those of the same dates at 12:00 PM are illustrated in Figure 5B, where solid, dashed, dotted lines, dash-dotted lines indicate the data of the date from 24 to 27, respectively. In order to confirm the effects on the path losses due to the atmospheric conditions and the accuracy of our simulation, the path losses measured from October 24 to October 27, 2017 at the Heuksando Rx station, are compared with the simulation as shown in Figure 6, where the super or duct atmospheric conditions occurred on most of the measurement dates. Figure 6 presents the real-time measured results at the same time interval of 30 seconds with the data points of 9997, which are specified by black dotted markers. Red and blue dotted markers indicate the measurement results for 1 hour before and after around 0:00 AM and 12:00 PM for each day, respectively. The two-hour

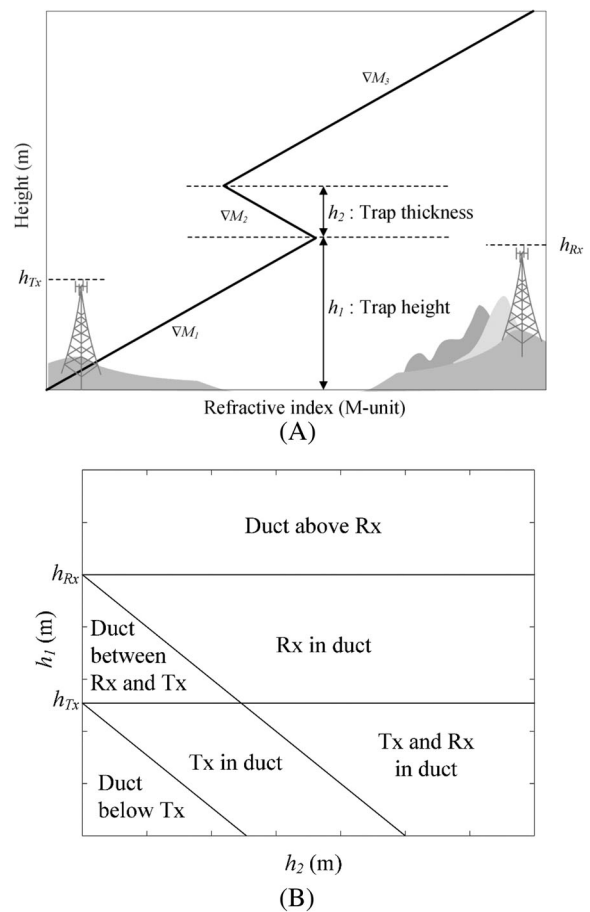


**FIGURE 7** The conventional trilinear model and the proposed duct map for the various duct types. A, Conventional trilinear modeling of the modified atmospheric refractivity for an arbitrary duct atmosphere. B, The proposed duct map including the information of the  $h_{Tx}$  and  $h_{Rx}$

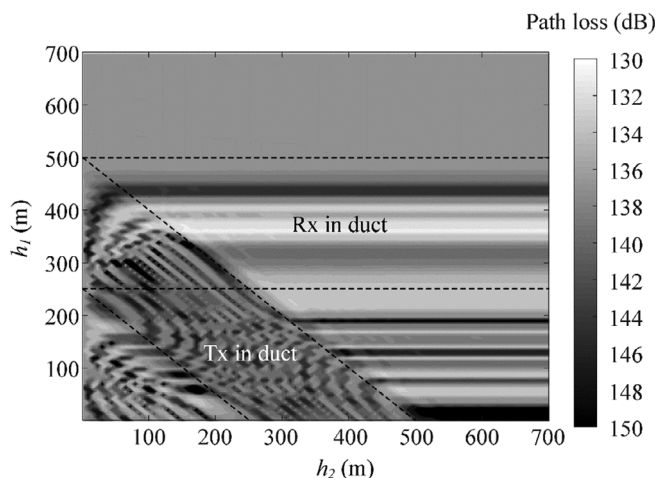
measured data around 0:00 AM and 12:00 PM were averaged for comparison with the simulations. The average of the measured data is 139.7 dB, which is consistent with a simulated path loss of 138.1 dB. The difference between measurement and

simulation are due to limitations of the AREPS software that do not support the system parameters such as a system noise, a total system input power, and the detailed range dependent refractivity. As expected, under the super or duct atmospheric conditions, a high-level signal reception with less path loss is observed in this case study. In the following chapter, we examine in more detail the effects of various duct phenomena with different trap thicknesses and heights.

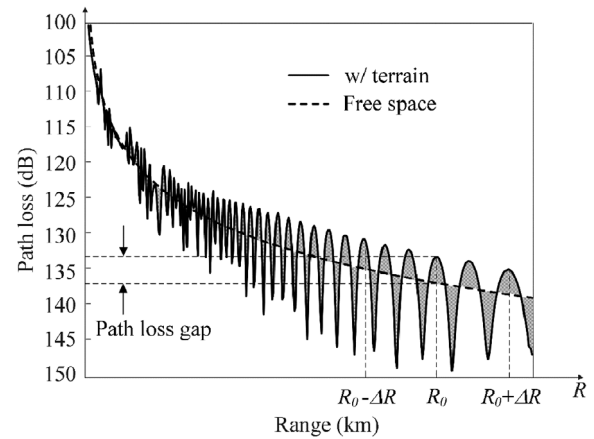
### 3 | PARAMETRIC STUDY AND ANALYSIS

Figure 7A shows the conventional trilinear modeling of  $M$  to represent the duct atmospheric conditions, which can be used to observe the effects of the duct on the path loss depending on various duct properties. To create arbitrary duct atmospheric conditions, the slope  $\nabla M_2$  of the second linear line has a negative value indicating the trap atmospheric condition that occurs at a height of  $h_1$  with a thickness of  $h_2$ , while the slopes  $\nabla M_1$  and  $\nabla M_3$  of the first and third linear lines are positive values. However, since this trilinear modeling of  $M$  does not contain the antennas' altitude information of the Tx ( $h_{Tx}$ ) and Rx ( $h_{Rx}$ ), it is not easy to examine the effect of the relationship between the duct shape ( $h_1$  and  $h_2$ ) and the antenna positions ( $h_{Tx}$  and  $h_{Rx}$ ) on the path loss. Therefore, we propose a novel duct map that can effectively estimate the abnormal wave propagation characteristics by including  $h_{Tx}$  and  $h_{Rx}$ , as shown in Figure 7B. In Figure 7B, both the  $\nabla M_1$  and  $\nabla M_3$  are 118 to make the normal atmospheric condition, and the  $\nabla M_2$  is the negative value of  $-118$  in order to model the duct atmosphere.

Figure 8 illustrates the resulting duct map with the path losses at the Rx with a flat ground, where  $h_{Tx}$  and  $h_{Rx}$  are 250 and 500 m, respectively. Here, the duct map clearly shows the relationship between the duct shape ( $h_1$  and  $h_2$ ) and the positions ( $h_{Tx}$  and  $h_{Rx}$ ), which exhibits significantly



**FIGURE 8** The duct map with the path losses at the Rx with a flat ground ( $h_{Tx} = 250$  m and  $h_{Rx} = 500$  m)



**FIGURE 9** Path loss in terms of the distance  $R$  between the Tx and Rx

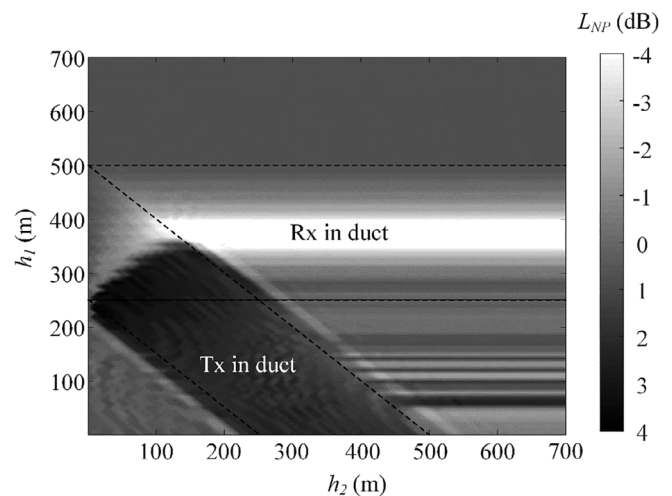


**FIGURE 10** The duct map of the average normalized path loss  $L_{NP}$  with a flat ground ( $h_{Tx} = 250$  m and  $h_{Rx} = 500$  m)

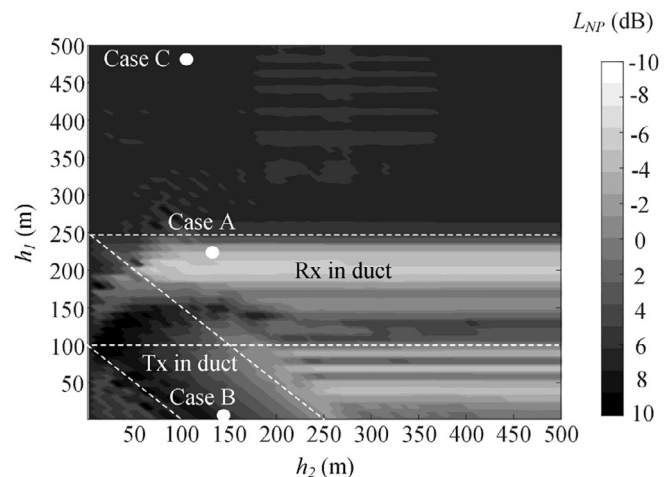


**FIGURE 11** The duct map of the average normalized path loss  $L_{NP}$  with the digital terrain elevation data (DTED) of Jeungdo-Heuksando coastal area ( $h_{Tx} = 100$  m and  $h_{Rx} = 249$  m)

different path losses depending on the area divided by the dashed lines. However, fluctuations in path losses according to  $h_1$  and  $h_2$  are observed due to EM properties such as the effect of ground reflections. The reason for fluctuations can be found more clearly by observing the path loss in terms of the distance  $R$  between the Tx and Rx, as shown in Figure 9. The path loss  $L_f$  (solid line) without the terrain data is gradually reduced by a square of the distance and can be calculated simply using the Friis equation<sup>19,23</sup> as follows:

$$L_f = \left(\frac{4\pi R}{\lambda}\right)^2, \quad (2)$$

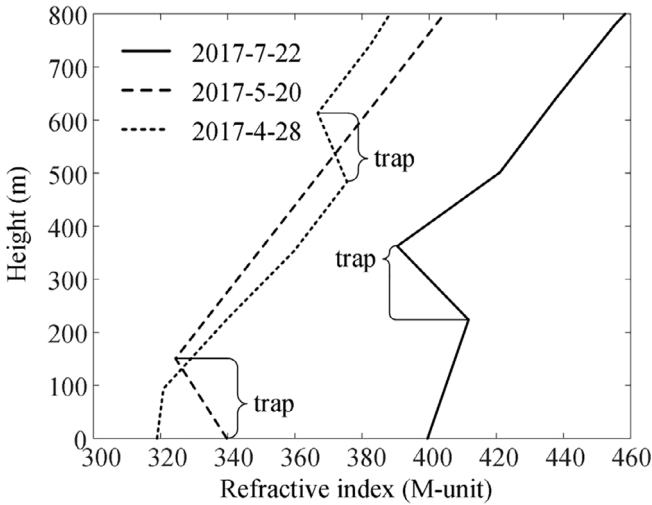


FIGURE 12 Modified atmospheric refractivity according to altitude depending on dates

where  $R$  is the distance from the Tx to Rx, and  $\lambda$  is wavelength. On the other hand, the simulated path loss with the terrain data is fluctuating by the reflections from terrain grounds, but the overall envelope of the path loss follows the trend of  $L_f$ . Therefore, in order to more clearly observe the duct effect, we propose to use the average normalized path loss  $L_{NP}$  defined as follows:

$$L_{NP} = \frac{\int_{R_0 - \Delta R_0}^{R_0 + \Delta R_0} (L_{Rx}(R) - L_f(R)) dR}{2\Delta R_0}, \quad (3)$$

where  $R_0$  is the actual distance between Tx and Rx, and  $L_{Rx}(R)$  is the path loss with the terrain data at a distance  $R$ . Then, the normalized path loss can be expressed as  $L_{Rx}(R) - L_f(R)$ , and the average normalized path loss  $L_{NP}$  can be obtained by averaging it from  $R_0 - \Delta R_0$  to  $R_0 + \Delta R_0$ .  $L_{NP}$  observes the deviations from free-space path losses where the terrain reflection effects are compensated, so that the duct effects can be seen more accurately. The re-calculated duct map with the average normalized path loss  $L_{NP}$  is shown in Figure 10. Abnormal wave propagations are examined when  $h_1$  and  $h_2$  are similar to  $h_{Tx}$  and  $h_{Rx}$ . In particular, the lowest  $L_{NP}$  of  $-7.35$  dB is observed when  $h_1 = 375$  m and  $h_2 = 149.3$  m, where  $h_{Tx}$  is slightly below the duct and  $h_{Rx}$  is in the duct. On the other hand, the highest  $L_{NP}$  of  $3.94$  dB is achieved at  $h_1 = 220$  m and  $h_2 = 22$  m, respectively, where  $h_{Tx}$  is in the duct and  $h_{Rx}$  is outside the duct. When  $h_1$  is much lower or higher than  $h_{Tx}$  and  $h_{Rx}$ , normal propagation characteristics are observed.

Finally, instead of the flat ground, the DTED in the Korean coastal area of Jeungdo-Heuksando is included in the AREPS simulation software to observe abnormal wave

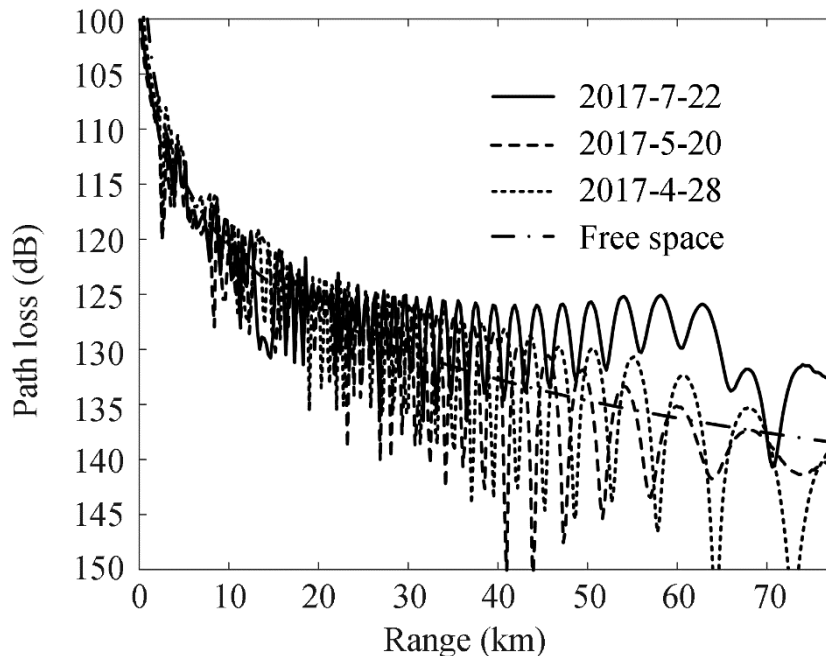


FIGURE 13 Simulation results of the path losses along the range depending on dates



propagations in various duct conditions between the Tx and Rx stations constructed for measurement, as shown in Figure 11. Now  $h_{Tx}$  is 100 m at Jeungdo, and  $h_{Rx}$  is 249 m at Heuksando. The duct map shows a very similar relationship between  $h_{Tx}$  and  $h_{Rx}$ , and  $h_1$  and  $h_2$ , with the results of the flat ground. In the resulting duct map, three representative duct conditions of Case A, Case B, and Case C in Figure 11 are investigated in more detail. In Case A, the elevated duct occurs with  $h_1 = 233$  m and  $h_2 = 139$  m, where the  $h_{Tx}$  is slightly below the  $h_1$  and  $h_{Rx}$  is in the duct. We find that this duct condition is most similar to the actual atmospheric refractive index of the weather database on July 22, 2017 from the Heuksando meteorological observatory in Figure 12. Case B is for another abnormal case, where  $h_{Tx}$  is in the duct while  $h_{Rx}$  is outside the duct. This duct condition is similar to the weather database on May 20, 2017 from the same forecast station in Figure 12. We also checked the duct case at the nearest meteorological observatory in Gwangju that is 72 km from Jeungdo. In Figure 12, Dashed line shows the modified refractivity indices for April 28, 2017 from Gwangju that is similar to Case C. For Case C, both  $h_{Tx}$  and  $h_{Rx}$  are outside the duct. Figure 13 represents the AREPS simulation results of the path losses along the range using real atmospheric conditions for Case A, Case B, and Case C, including the DTED of the Jeungdo-Heuksando. The path loss for Case A is indicated by the solid line and is 132.3 dB at the Rx point. The abnormal radio wave propagation delivers a large amount of energy to the Rx compared to the free space. On the other hand, the dashed line for Case B shows a higher path loss of 140.1 dB at the Rx point. This is because most of the energy from Tx is trapped in the duct, and Rx is placed outside the duct, making it difficult to receive the energy by wave propagation. The path loss for Case C is 138.8 dB at the Rx point, which is similar to free space path loss.

## 4 | CONCLUSION

We have investigated the path losses of the wave propagation between the Jeungdo and Heuksando transceivers in Korea coastal areas using the AREPS simulation software based on the weather database of the Heuksando weather forecast station and the digital terrain elevation data. Based on the simulated results, a novel duct map was proposed that can effectively predict the abnormal wave propagation characteristics according to the modified refractive index. We first confirmed the effects of the duct atmosphere on the wave propagation by comparing the measured and simulated data, and the averages of the measured and simulated path losses were 139.7 and 138.1 dB from October 24 to 27 in 2017 at the Heuksando Rx station. In order to certify the proposed duct map, two representative refractive indices causing abnormal wave propagations were then attained from the 2017 weather database, which are most similar to

the resulting refractive indices of the duct map. For the first case, the path loss was 132.3 dB at the Rx point, and the abnormal radio wave propagation delivers a large amount of energy to the Rx compared to the free space. On the other hand, a higher path loss of 140.1 dB was obtained at the Rx point for the other case, where most of the energy from Tx was trapped in the duct, and Rx was placed outside the duct, making it difficult to receive the energy by wave propagation. This is because most of the energy from Tx was trapped in the duct, and Rx was placed outside the duct, making it difficult to receive the energy by wave propagation. The results demonstrated that the prediction of an abnormal radio wave propagation can be accomplished through the observation of the proposed duct map and the height parameters of Rx and Tx in comparison to the altitude of the duct could induce considerably distinct path loss characteristics.

## ACKNOWLEDGMENTS

This work was supported by a grant-in-aid of HANWHA SYSTEMS and Institute for Information & communications Technology Promotion (IITP) grant funded by the Korea government (MSIP) (No.2017-0-00066, Development of time-space based spectrum engineering technologies for the preemptive using of frequency).

## ORCID

Hosung Choo  <https://orcid.org/0000-0002-8409-6964>

## REFERENCES

- [1] Rappaport TS, MacCartney GR, Molisch AF, Mellios E, Zhang J. Overview of millimeter wave communications for fifth-generation (5G) wireless networks—with a focus on propagation models. *IEEE Trans Antennas Propag.* 2017;65(12):6213-6230.
- [2] Kim JY, Chun DW, Ryu CJ, Lee HY. Optimization methodology of multiple air hole effects in substrate integrated waveguide applications. *J Electromagn Eng Sci.* 2018;18(3):160-168.
- [3] Jeon HG, Shin SM, Hwang T, Kang CE. Reverse link capacity analysis of a CDMA cellular system with mixed cell sizes. *IEEE Trans Veh Technol.* 2000;49(6):2158-2163.
- [4] Valtr P, Pechac P. The influence of horizontally variable refractive index height profile on radio horizon range. *IEEE Antennas Wirel Propag Lett.* 2005;4:489-491.
- [5] Karimian A, Yardim C, Gerstoft P, Hodgkiss WS, Barrios AE. Refractivity estimation from sea clutter: an invited review. *Radio Sci.* 2011;46(6):1-16.
- [6] Wagner M, Gerstoft P, Rogers T. Estimating refractivity from propagation loss in turbulent media. *Radio Sci.* 2016;51(12):1876-1894.
- [7] *Recommendation ITU-R P.453-13: The Radio Refractive Index: Its Formula and Refractivity Data.* International Telecommunication Union; 2017.



- [8] Kim C, Park YB. Prediction of electromagnetic wave propagation in space environments based on geometrical optics. *J Electromagn Eng Sci*. 2017;17(3):165-167.
- [9] Abdulhadi A, Raed AAA, Steve MRJ, Hussain AA. New methodology for predicting vertical atmospheric profile and propagation parameters in subtropical Arabian Gulf Region. *IEEE Trans Antennas Propag*. 2015;63(9):4057-4068.
- [10] Dinc E, Akan OB. Channel model for the surface ducts: large-scale path-loss, delay spread, and AOA. *IEEE Trans Antennas Propag*. 2015;63(6):2728-2738.
- [11] Sirkova I. Propagation factor and path loss simulation results for two rough surface reflection coefficients applied to the microwave ducting propagation over the sea. *Prog Electromagn Res*. 2011; 17:151-166.
- [12] Shi Y, Yang KD, Yang YX, Ma YL. Experimental verification of effect of horizontal inhomogeneity of evaporation duct on electromagnetic wave propagation. *Chin Phys B*. 2015;24(4):044102.
- [13] Dinc E, Akan OB. Beyond-line-of-sight communications with ducting layer. *IEEE Commun Mag*. 2014;52(10):37-43.
- [14] Bean BR, Thayer GD. Models of the atmospheric radio refractive index. *Proc IRE*. 1959;47(5):740-755.
- [15] Sirkova I. Brief review on PE method application to propagation channel modeling in sea environment. *Cent Eur J Eng*. 2012;2(1):19-38.
- [16] Pozderac J, Johnson J, Yardim C, et al. X-band beacon-receiver array evaporation duct height estimation. *IEEE Trans Antennas Propag*. 2018;66(5):2545-2556.
- [17] Lin LK, Zhao ZW, Zhang YR, Zhu QL. Tropospheric refractivity profiling based on refractivity profile model using single ground-based global positioning system. *IET Radar Sonar Navig*. 2011;5(1):7-11.
- [18] Norman RJ, Marshall JL, Rohm W, et al. Simulating the impact of refractive transverse gradients resulting from a severe troposphere weather event on GPS signal propagation. *IEEE J Sel Top Appl Earth Observ*. 2015;8(1):418-424.
- [19] Son HK, Kim JH, Kim CY. Analysis of radio interference through ducting for 2.5 GHz WiMAX service. *J Electromagn Eng Sci*. 2012;12(1):94-100.
- [20] *Advanced Refractive Prediction System (AREPS). Ver. 3.6*. San Diego, California: The Space and Naval Warfare System; 2005.
- [21] Ozlem O, Gokhan A, Mustafa K, Levent S. PETOOL: MATLAB-based one-way and two-way split-step parabolic equation tool for radiowave propagation over variable terrain. *Comput Phys Commun*. 2011;182:2638-2654.
- [22] Zhang P, Bai L, Wu Z, Guo L. Applying the parabolic equation to tropospheric groundwave propagation: a review of recent achievements and significant milestones. *IEEE Antennas Propag Mag*. 2016;58(3):31-44.
- [23] *Recommendation ITU-R P.525-4: Calculation of Free-Space Attenuation*. International Telecommunication Union; 2019.

**How to cite this article:** Wang S, Lim TH, Chong YJ, Ko J, Park YB, Choo H. Estimation of abnormal wave propagation by a novel duct map based on the average normalized path loss. *Microw Opt Technol Lett*. 2020;62:1662–1670. <https://doi.org/10.1002/mop.32205>